13th World Conference on Earthquake Engineering
Vancouver, B.C., Canada
August 1- 6, 2004
Paper No. 2890

# EFFECTS OF MULTI-DIRECTIONAL CYCLIC SHEAR ON THE POST-EARTHQUAKE SETTLEMENT OF GROUND

Hiroshi MATSUDA[1], Haruhiko SHINOZAKI[2], Naoki OKADA[3], Kouichi TAKAMIYA[4] and Keishi SHINYAMA[5]

## SUMMARY

The effects of direction of cyclic shear on the properties of saturated sandy soil such as vertical effective stress reduction during earthquake, post-earthquake settlement and shear strength were investigated by using the multi-directional cyclic simple shear test apparatus. As a result, it is found that these properties are affected by the multi-directional cyclic shear compared with single-directional shear and that the granulated blast furnace slag (GBFS), which is substituted for a natural sand, shows less vertical effective stress reduction and less settlement, hence higher shear strength than the natural sand.

## INTRODUCTION

The direction of seismic acceleration in the ground is not constant but multi-directional. Fig.1 shows the orbit of shear strain calculated from the time history of acceleration in Hyogo-ken Nanbu Earthqake, 1995.1.17. [1] From Fig.1, it is seen that the shear strain occurs in a predominant direction but rather elliptically.

Although many studies on the effective stress reduction and the settlement of the ground induced by the earthquake have been carried out, almost all the studies focused on the properties induced by the single directional shear. For the post earthquake settlement of the ground, conflicting results have been reported. [2][3] This is partly due to that the effect of the direction of cyclic shear on the settlement of sandy soil ground is not clarified.

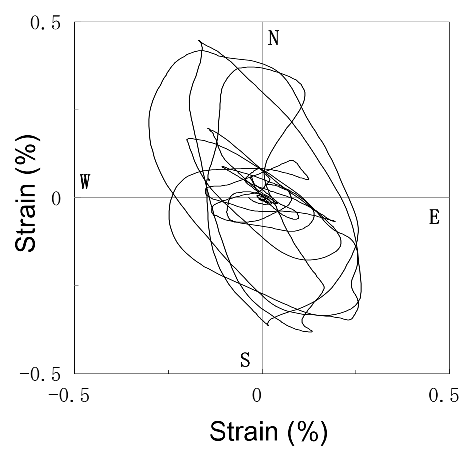


Fig.1 Orbit of shear strain in the ground measured at Hyogo-ken Nanbu Earthquake, 1995.1.17.

[1] Professor, Yamaguchi University, Japan
[2] PhD Student, Yamaguchi University, Japan (Nippon Steel Co. Ltd.)
[3] Graduate Student, Yamaguchi University, Japan
[4] Assistant, Yamaguchi University, Japan
[5] Graduate Student, Yamaguchi University, Japan

On the other hand, because of the environmental conservation or the ecological preservation in recent years, it became more difficult to acquire a lot of natural sand with high shear strength and high permeability. As an alternative natural sand, the granulated blast furnace slag (GBFS) is considered to be one of promising materials.

In this paper, by using the multi-directional cyclic simple shear test apparatus, the effects of cyclic shear direction on the effective vertical stress reduction during cyclic shear, the settlement and the shear strength after cyclic shear were investigated for various saturated sandy materials.

## APPARATUS AND SAMPLES

### Apparatus and test procedures

Fig.2 shows the outline of the multi-directional cyclic simple shear test apparatus. This apparatus can give any types of cyclic shear strain to the bottom face of specimen (Diameter and thickness are φ=75mm, H=20mm, respectively), from orthogonal two directions, independently by the electro-hydraulic servo systems. Vertical stress is applied to the specimen by the aero-servo system.

A series of tests was carried out as follows.

Saturated sands were poured into the shear box at the relative density Dr=70%, then the specimens were consolidated for 15 minutes under the vertical stress $\sigma_v$'= 49 kPa.

During the cyclic shear, the vertical displacement of specimen was restricted to keep the volume of specimen constant.

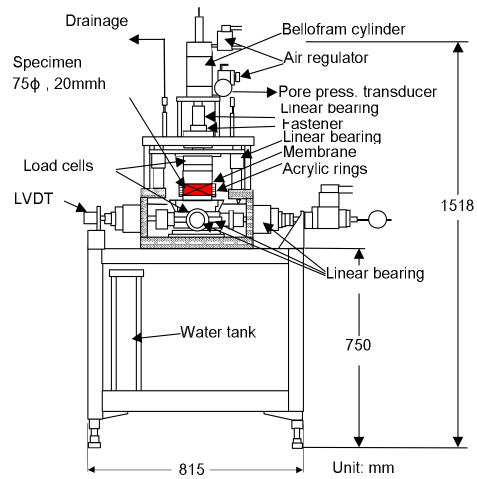


Fig.2 Multi-directional cyclic simple shear test apparatus.

After the cyclic shear, the specimens were re-consolidated for 15 minutes under the vertical stress $\sigma_v$'=49kPa. Then the vertical settlement was measured with time. Furthermore, to clarify the influence of cyclic shear on the static shear strength of saturated sand, static simple shear tests (CU) were also performed before and after cyclic shear, in which shear strain rate was set as 1%/min.

The wave form of applied shear strain is sinusoidal which is obtained by equation (1) and three patterns of shear strain as CASE1, CASE 2 and CASE 3 were used.

$$\gamma = \gamma_{\max} \sin(\frac{T}{2\pi} t) \qquad (1)$$

where $\gamma$ is the shear strain amplitude, $\gamma_{max}$ is the maximum shear strain amplitude and T is the period of cyclic shear.

1) CASE 1: Shear strain is applied to the specimen in X-direction. (Single-directional shear)
2) CASE 2: Shear strain is applied to the specimen in Y-direction. (Single-directional shear)
3) CASE 3: Shear strain is applied to the specimen simultaneously in both X and Y directions with the predetermined phase difference. When the phase difference is π/2 in radian, the loading is called gyratory shear. (Multi-directional shear)

In this paper, Y axis intersects perpendicularly to X axis at the center of horizontal bottom surface of the specimen. The period of sinusoidal shear strain was set as T=2s, and the shear strain amplitude and the number of strain cycles n were set in the range from γ=0.1% to 1%, and n= 5 and n=15, respectively.

Fig.3 shows shear patterns and a typical deformation of specimens, conceptually.

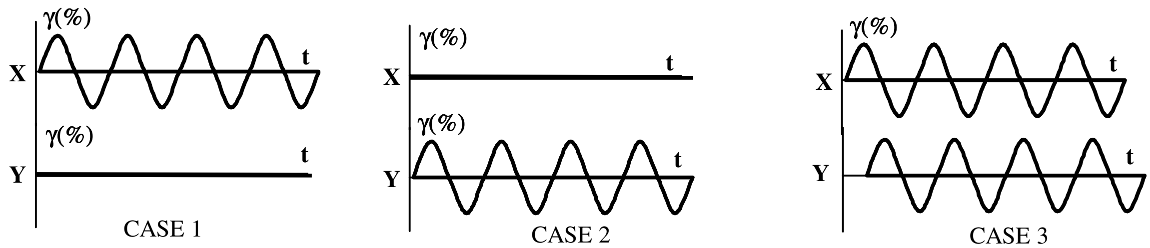


Fig.3 (a) Shear waves.

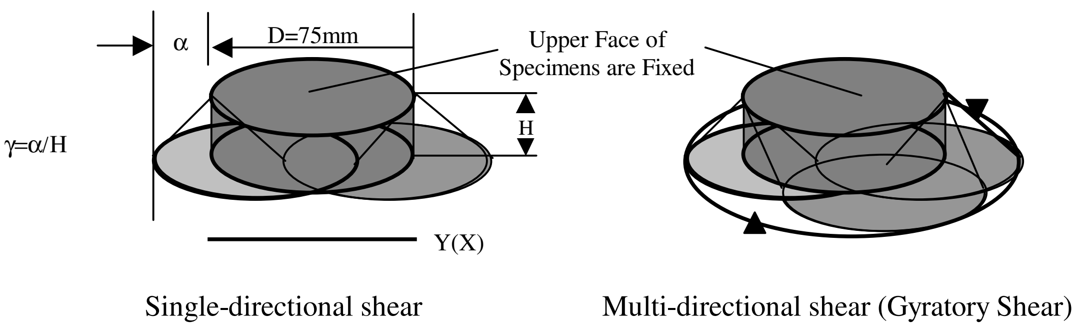


Fig.3 (b) Typical deformation of specimen.

**Sample and specimen**

In this study, Toyoura sand, Genkai sand, and granulated blast furnace slag were used as a sample. Toyoura sand is the standard sand as a natural geo-material in Japan and Genkai sand is a kind of typical natural sea sand. On the other hand, granulated blast furnace slag (GBFS) is by-product, which is granulated by rapid water-cooling of molten blast furnace slag in the iron making process and mainly used to produce blast furnace cement in Japan. As a geo-material, GBFS has particular properties such as light-weight ($\gamma_t$ =13kN/m$^3$) high internal-friction angle ($\varphi$=35) and high permeability (k=10$^{-1}$-10$^{-2}$cm/s) . Because of these properties, a guideline for using GBFS in the port structure constructions [4] has been published in 1989 and situated as a useful recycle material in Japanese technical standard for port and harbor facilities. (revised in April 1999)

Physical properties and grain distribution curves of each material are shown in Table 1 and Fig.4, respectively.

Table 1 Physical properties of sample.

| Materials | Specific gravity $\rho_s$ (g/cm$^3$) | Maximum void ratio $e_{max}$ | Minimum void ratio $e_{min}$ |
|---|---|---|---|
| GBFS | 2.702 | 1.413 | 0.904 |
| Genkai sand | 2.678 | 0.827 | 0.516 |
| Toyoura sand | 2.637 | 0.991 | 0.630 |

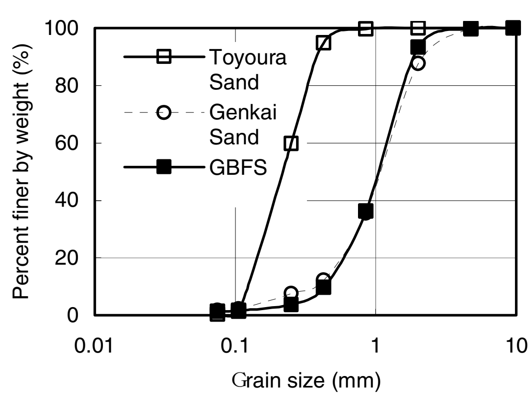


Fig.4 Grain size distribution curves of sample.

## EFFECTS OF CYCLIC SHEAR DIRECTION

### Change in the vertical effective stress

Figs.5 (a) (b) show the change of vertical effective stress, for Toyoura sand with Dr=70%. Fig.5(a) shows the results for the case of multi-directional shear strain amplitude $\gamma_{max}$ =0.5% and the single-directional shear strain amplitude $\gamma_{max}$ =0.5-1.0%. Fig.5(b) shows for the case of multi-directional shear strain amplitude $\gamma_{max}$ =1.0% and the single-directional shear strain amplitude $\gamma_{max}$ =1.5-2.0%. Vertical effective stress decreases with number of strain cycles and the vertical effective stress reduction in the case of multi-directional shear is larger than that of single-directional shear.

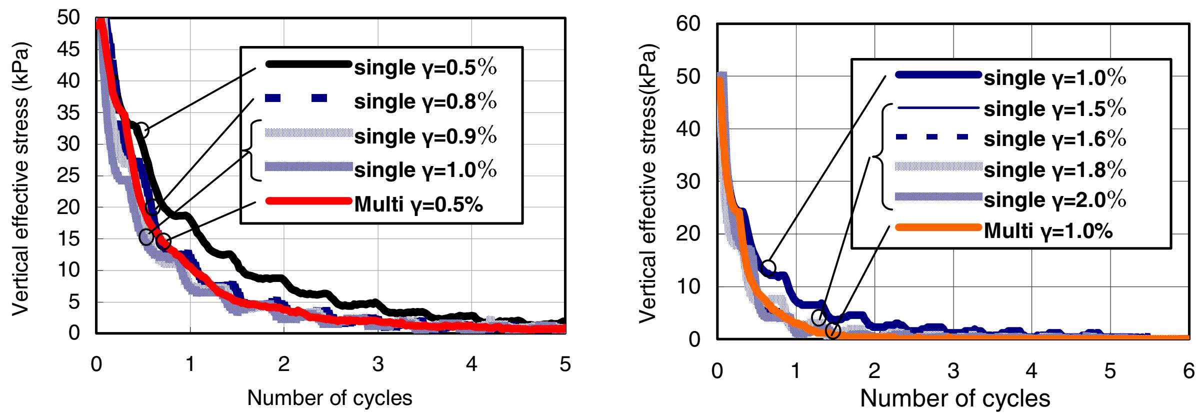


(a) Multi-directional shear strain amplitude $\gamma_{max}$ =0.5% and single directional shear strain amplitude $\gamma_{max}$ = 0.5-1.0%.

(b) Multi-directional shear strain amplitude $\gamma_{max}$ =1.0% and single directional shear strain amplitude $\gamma_{max}$ = 1.5-2.0%.

Fig.5 Changes in vertical effective stress for Toyoura sand.

It is interesting that in the case of single-directional shear, the curves fluctuate in comparison with the case of multi-directional shear in which the effective stress smoothly reduces. The reason might be that in the case of single-directional shear, each particle moves two or three dimensionally running over other particles, but in the case of multi-directional shear, each particle moves only vertically by keeping their relative positions between particles. Comparing Figs.5(a) and 5(b), in the case of single-directional shear, the larger the shear strain amplitude, the larger the vertical effective stress reduces. As for the vertical effective stress reduction, the equivalent single-directional shear strain amplitude to the multi-directional shear strain amplitude of $\gamma_{max}$ =0.5% can be evaluated to be 0.8-1.0% (About 1.6-2.0 times of the multi-directional shear strain amplitude,) and multi-directional shear strain amplitude $\gamma_{max}$ =1.0% can be evaluated to be 1.5-2.0% (About 1.5-2.0 times of  the multi-directional shear strain amplitude.).

### Settlement in the re-consolidation stage after cyclic shear

Fig.6 and Fig.7 show vertical settlement in strain at the re-consolidation stage after cyclic shear. Fig.6 shows the results for the case of multi-directional shear strain $\gamma_{max}$= 0.5% and the single directional shear strain $\gamma_{max}$ =0.5-1.0%. Fig.7 also shows for the multi-directional shear strain $\gamma_{max}$=1.0% and single-directional shear $\gamma_{max}$ =1.0-2.0%, respectively. Figs.6(a),7(a) and 6(b),7(b) show the results for the number of cycles n=5 and n=15, respectively.

The settlements increase with the shear strain amplitude but the rate of increase reduces with the number of cycles. As for the settlement, the equivalent single-directional shear strain amplitude to the multi-directional shear strain amplitude $\gamma_{max}$ = 0.5% can be evaluated to be 0.9%. (About 1.8 times of multi-directional shear strain amplitude.)

Comparing Figs.7(a) and 7(b), the differences reduce with the number of cycles. Equivalent single-directional shear strain amplitude to the multi-directional shear strain amplitude $\gamma_{max}$=1.0% can be evaluated to be 1.5-2.0%. (About 1.5-2.0 times of single-directional shear strain amplitude.)

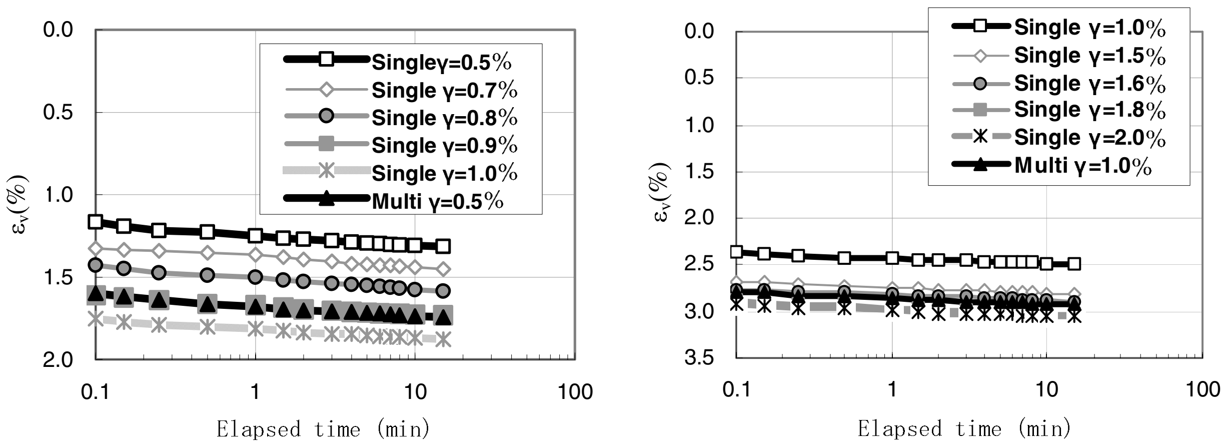


(a) (b)

Fig.6 Vertical settlement $\varepsilon_v$ at the re-consolidation stage after cyclic shear for Toyoura sand.

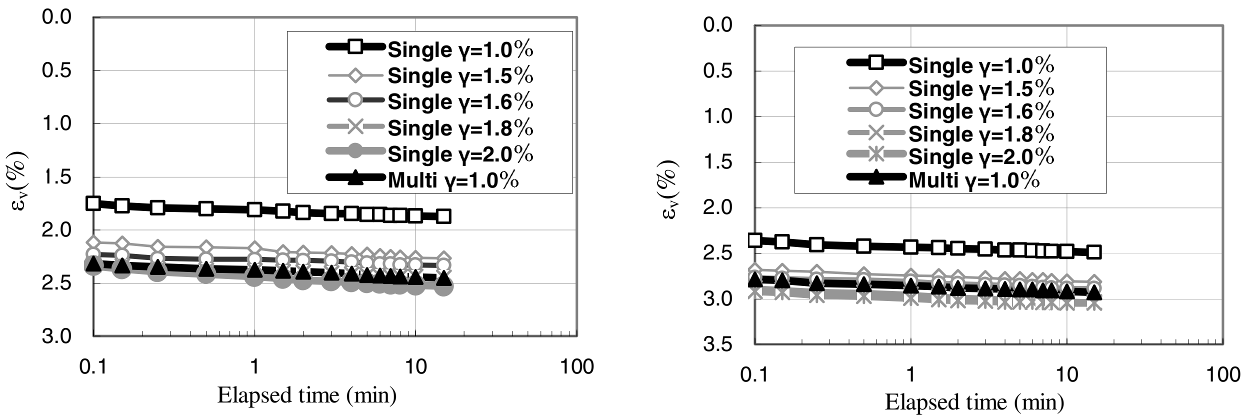


(a) (b)

Fig.7 Vertical settlement $\varepsilon_v$ at the re-consolidation stage after cyclic shear for Toyoura sand.

Table 2 Equivalent single-directional shear strain amplitude to multi-directional shear for the effective stress reduction and settlement.

| Shear strain amplitude $\gamma$ of Multi-directional shear | | Equivalent single shear strain amplitude to multi-directional shear | |
|---|---|---|---|
| | | n=5 | n=15 |
| $\gamma$ =0.5% | Effective stress reduction | 0.8-1.0% | - |
| | Settlement | 0.9% | 0.9% |
| $\gamma$=1.0% | Effective stress reduction | 1.5-2.0% | - |
| | Settlement | 1.8-2.0% | 1.5-2.0% |

Above mentioned results are summarized in Table 2.

Fig.8 shows settlement in strain $\varepsilon_v$ induced in the re-consolidation stage. From Fig.8, the settlement increases in proportional with the cyclic shear strain amplitude for n=5 and n=15 and equivalent single directional shear strain amplitude to the multi-directional shear can be evaluated to be about 1.5-2.0 times of the single-directional shear strain amplitude.

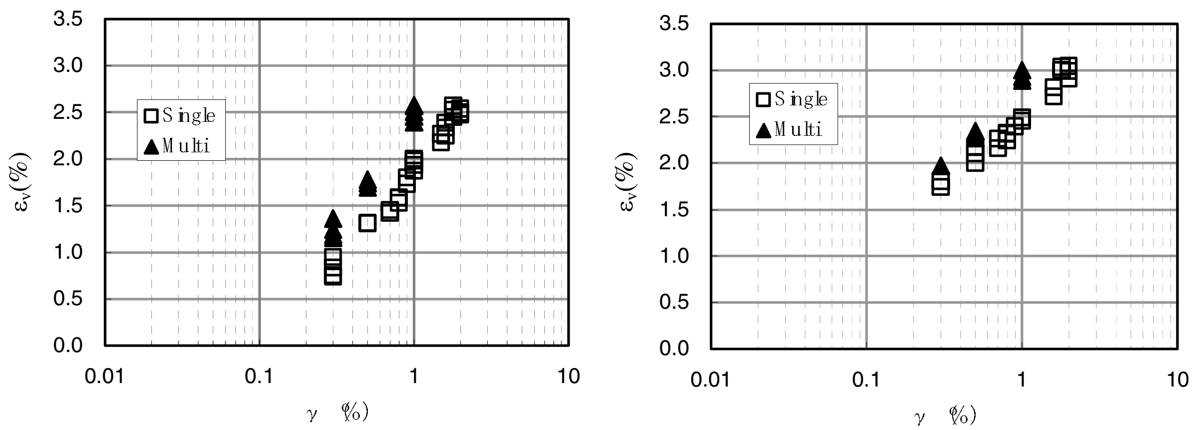


(a) n = 5 (b) n =15

Fig.8 Vertical strain $\varepsilon_v$ in the re-consolidation stage for Toyoura sand.

## COMPARISON BETWEEN THE GBFS AND NATURAL SAND

### Effective stress reduction of GBFS and natural sand

Fig.9 shows changes of vertical effective stress for the case of GBFS which was compacted to the relative density Dr=70%. Vertical effective stress reduction becomes larger with cyclic shear strain amplitude. It is apparent that the vertical stress reduction in the case of single-directional shear strain (X direction) is almost the same as that of Y direction. Vertical effective stress reduction in the case of multi-directional shear is larger than that of single directional shear. This tendency is almost the same as Toyoura sand.(Fig.5)

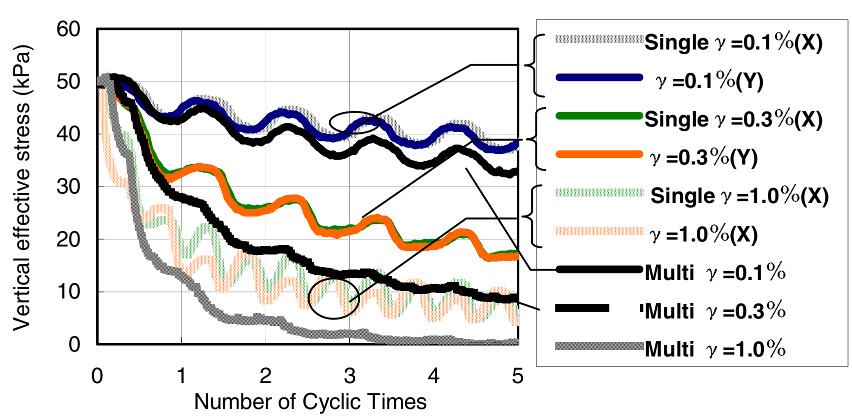


Fig.9 Changes of vertical effective stress for GBFS.

Fig.10 shows the relations between the effective stress reduction ratio which is defined as $\left|\Delta\sigma_v / \sigma'_{vo}\right|$ and the cyclic shear strain amplitude γ.

As for the effective stress reduction ratio $\left|\Delta\sigma_v / \sigma'_{vo}\right|$, GBFS <Genkai sand <Toyoura sand in sequence is obtained. These results might be due to the difference in the material property, for example, particle

shape, particle shear strength etc. Particularly, it is well known that the particle shape of GBFS is rough and internal friction angle φ is higher than those of other materials.

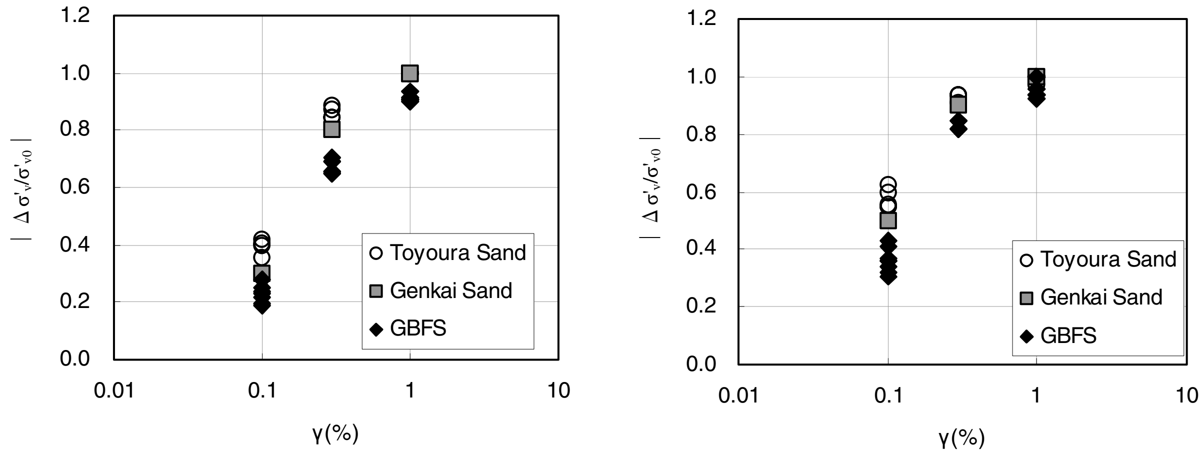


(a)Single-directional shear strain (b)Multi-directional shear strain

Fig.10 Relations between the effective stress reduction ratio $|\Delta\sigma_v / \sigma'_{vo}|$ and cyclic shear strain amplitude $\gamma_{\max}$ .

**Settlement in re-consolidation stage for GBFS and natural sand**

Fig.11 shows the change of vertical strain $\varepsilon_v$ at the re-consolidation stage after cyclic shear for GBFS with Dr=70%. The vertical strain $\varepsilon_v$ becomes larger with cyclic shear strain amplitude.

It is apparent that the vertical settlement in strain $\varepsilon_v$ for both cases of single-direction shear strain X and that of Y direction are almost the same. The vertical strain $\varepsilon_v$ in the case of multi-directional shear is larger than that of single directional shear. These tendencies are the same as Toyoura sand as shown in Figs.6 and 7.

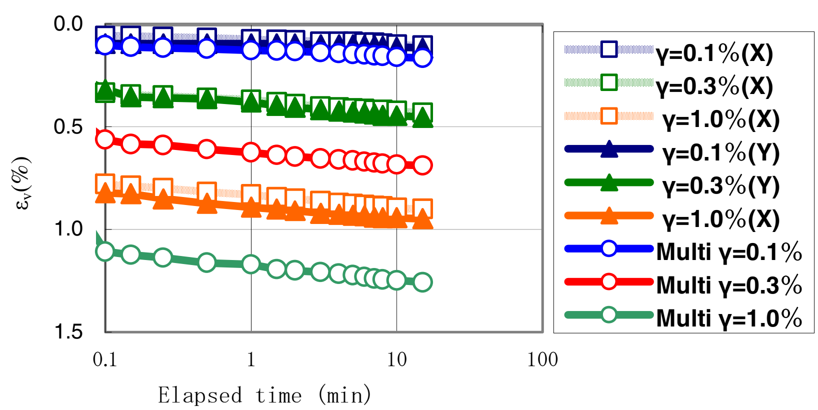


Fig.11 Vertical strain $\varepsilon_v$ at the re-consolidation stage after cyclic shear of n=5. (GBFS)

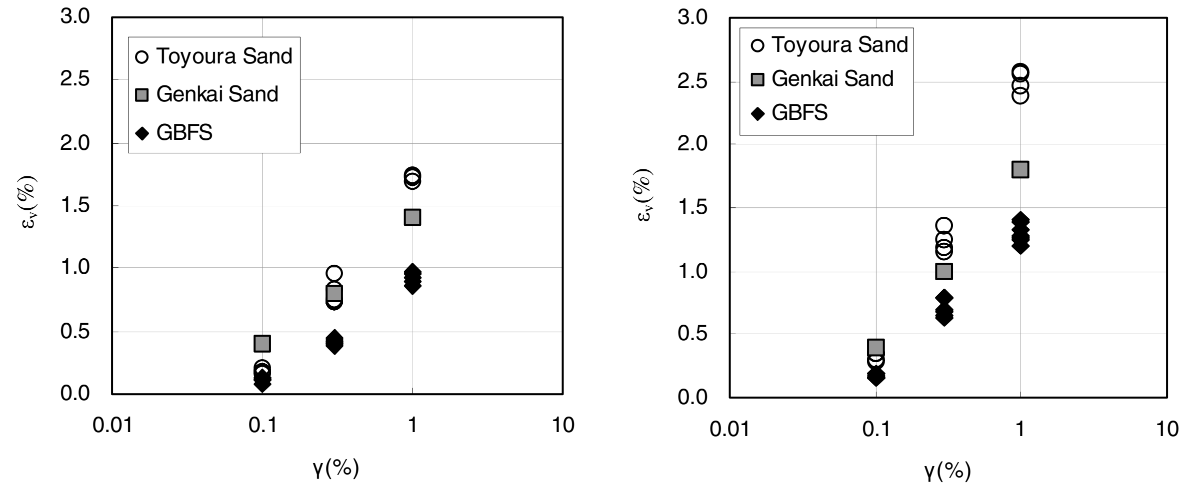


(a)Single-directional shear strain. (b)Multi-directional shear strain.

Fig.12 Relations between $\varepsilon_v$ in the re-consolidation stage and cyclic shear strain amplitude $\gamma$.

Fig.12 shows the relation between the vertical strain $\varepsilon_v$ induced in the re-consolidation stage and the cyclic shear strain amplitude.

As for the vertical strain $\varepsilon_v$, GBFS <Genkai sand <Toyoura sand in sequence is obtained which is almost the same as the results for the effective stress reduction ratio $|\Delta\sigma_v / \sigma'_{vo}|$. (Fig.10)

Fig.13 shows the relations between effective stress reduction ratio $|\Delta\sigma_v / \sigma'_{vo}|$ and the vertical strain $\varepsilon_v$ at the re-consolidation stage. When $|\Delta\sigma_v / \sigma'_{vo}| < 1.0$, all plots are on the same line irrespective of samples. This means that the post earthquake settlement can be predicted from the effective stress reduction ratio $|\Delta\sigma_v / \sigma'_{vo}|$.

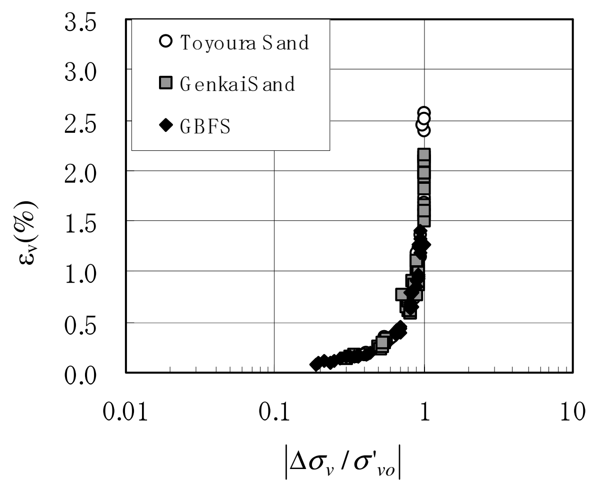


Fig.13 Relation between $|\Delta\sigma_v / \sigma'_{vo}|$ and $\varepsilon_v$ in the re-consolidation stage.

**Shear strength of GBFS and natural sand pre-subjected to cyclic shear**

Fig.14(a) shows the result of static simple shear test (CU), which was performed after the re-consolidation stage following the cyclic shear. In a test, the maximum shear strain was limited to 15% because the shear stress did not show a maximum value. It is seen that the larger the cyclic shear strain amplitude, the larger the shear stress becomes.

Fig.14(b) shows the change of effective vertical stress with the shear strain. The effective vertical stress once decreases temporarily and then increases. This might be due to the dilatancy of the sample.

Fig.15 shows the relations between the shear stress at the shear strain of 15% and the change of void ratio $\Delta e$ induced in the reconsolidation stage. In the figure, $\Delta e=0$ means that the specimen has no experience of cyclic shear. It is seen that the shear strength for GBFS is higher than that of Genkai sand or Toyoura sand.

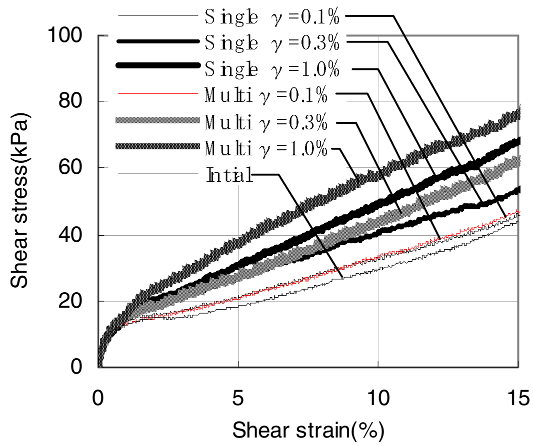


(a) Relation between shear strain and shear stress.

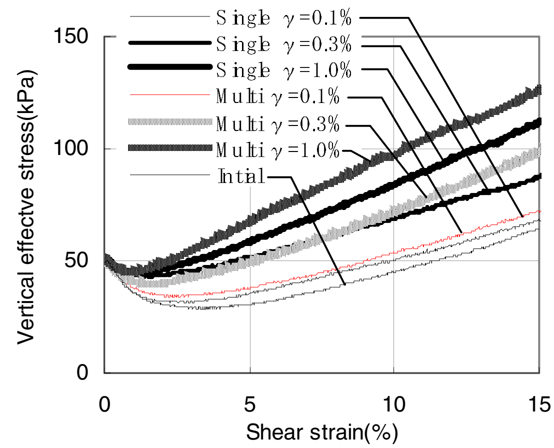


(b) Relation between shear strain and $\sigma_v'$.

Fig.14 Relations among shear stress, vertical effective stress $\sigma_v'$ and shear strain.

Fig.16 shows the relations between shear strength τ and the effective stress reduction ratio $\left|\Delta\sigma_v / \sigma'_{vo}\right|$. When $\left|\Delta\sigma_v / \sigma'_{vo}\right|$<1.0, the shear strength τ for GBFS is located at the highest position compared with other sands used in this study.

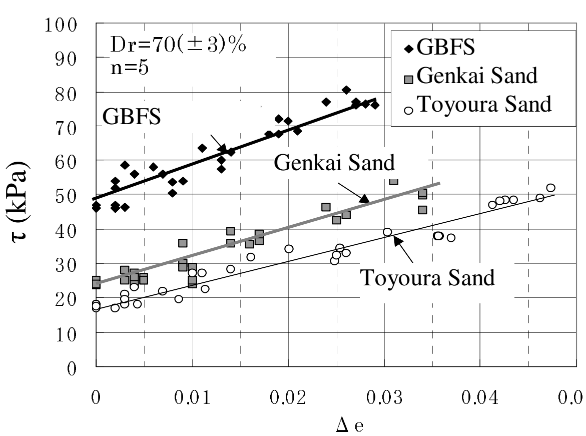


Fig.15 Relations between shear strength and $\Delta e$ in the re-consolidation stage.

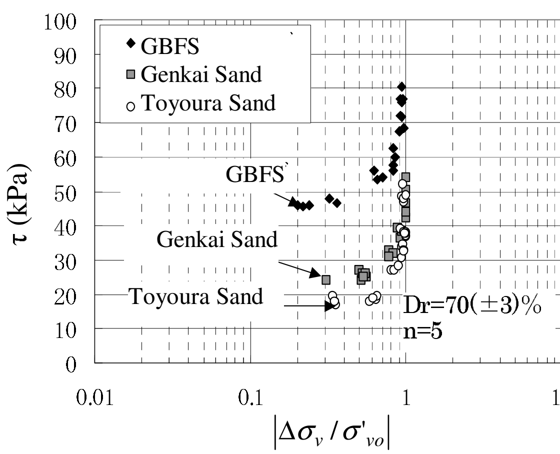


Fig.16 Relations between shear strength and effective stress reduction ratio $\left|\Delta\sigma_v / \sigma'_{vo}\right|$.

Fig.17 shows the relations between the shear strength ratio $\tau/\tau_s$ and Δe, where $\tau_s$ is the shear strength without the cyclic shear history. All plots are on the same line, and this means that $\tau/\tau_s$ is determined by the change of the void ratio Δe induced by the cyclic shear.

## CONCLUSIONS

In this study, by using the multi-directional cyclic simple shear test apparatus, effects of shear directions on the basic geotechnical properties such as effective vertical stress reduction during cyclic shear, settlement and shear strength after cyclic shear, were investigated for saturated sands including Granulated blast furnace slag. In conclusion, following results were obtained.

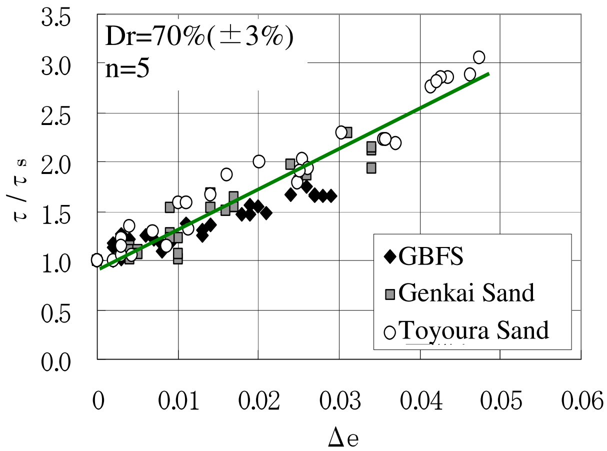


Fig.17 Relations between shear strength ratio $\tau/\tau_s$ and $\Delta e$.

(1) The vertical effective stress reduction $\Delta\sigma_v$' and the vertical strain $\varepsilon_v$ in the stage of re-consolidation increase with cyclic shear strain amplitude and with the number of cycles. In the case of multi-directional shear, their value is larger than that of single-directional shear.
(2) The multi-directional shear strain amplitude, for the vertical effective stress reduction $\Delta\sigma_v$' and vertical strain $\varepsilon_{v,}$ can be evaluated to be equivalent to 1.5-2.0 times of single-directional shear strain amplitude.
(3) GBFS shows less vertical effective stress reduction during cyclic shear and less vertical strain during re-consolidation after cyclic shear compared with the natural sand.
(4) GBFS shows higher shear strength than the natural sand.
(5) A unique relation between the settlement in the re-consolidation stage after cyclic shear and effective vertical stress reduction was observed.
(6) Shear strength ratio $\tau/\tau_s$ is determined by the change of the void ratio induced by the cyclic shear.

Since this study was carried out under the limited shear conditions in which the idealized multi-directional shear strain was applied to the specimen, further studies might be necessary under the various conditions including the elliptical shear condition and also the wide range of cyclic shear strain amplitude. In addition, GBFS, which is the artificial sand, has latent hydraulic property, so in the solidification process of GBFS, the similar investigations as in this study should be performed.

## REFERENCES


1. Matsuda H., Yamamoto T. and Sakuradani K., "The influence for settlement of clay and sand by the direction of cyclic shear", 26th Symposium of Earthquake Engineering in Japan, pp.605-608, 2001.8.
2. Nagase H. and Ishihara K., "Liquefaction-Induced compaction and settlement of sand during earthquakes", Soil and Foundations, Vol.28, No.1, pp.65-76, 1998.
3. Pyke R., Seed H.B., Chan C. K., "Settlement of sands under multi-directional shaking", Journal of the Geotechnical Engineering Division, Vol.101, No.GT4, pp.379-398, 1975.
4. Coastal Development and Institute of Technology and Nippon Slag Association, "Guideline of granulated blast furnace slag for port construction", 1989.8.
5. The Japan port and harbor association, "Technical standards and commentaries for port and harbor facilities in Japan", 1999.4.